

Variation of pairing correlations caused by nuclear rotation

S. Tazaki, K. Muramatsu, and R. Hayakawa

Department of Applied Physics, Fukuoka University, Fukuoka, 814-01, Japan

M. Hasegawa

Laboratory of Physics, Fukuoka Dental College, Fukuoka, 814-01, Japan

(Received 23 February 1990)

The interplay between nuclear rotation and the pairing correlations is studied in the single- j shell model space with $j = \frac{13}{2}$. For this study, we employ both the cranking model and the particle-rotor model, the Hamiltonians of which are exactly diagonalized to avoid the ambiguity of the number-nonconserving pair field approximation. The discussions on the merit of the two models show that the particle-rotor model is more reliable than the cranking model. Through the investigations of the spin alignments, the pairing energy gap, and the wave functions, it is shown that the pairing vibrational modes play very important roles. The processes of the collapse of nucleon pairs due to the nuclear rotation are also discussed.

I. INTRODUCTION

The study of the pairing correlations in rapidly rotating nuclei has been stimulated by recent experimental development. The newly discussed point was how the pairing correlations vary their roles as the rotational frequency ω increases. This subject has been investigated by various methods which intend to overcome the defect of the well-known number nonconservation in the mean-field approximation of the Hartree-Fock-Bogolyubov (HFB) (or BCS); those are the generator-coordinate method (GCM),^{1,2} particle-number projection method,³⁻⁵ random-phase approximation (RPA),⁶⁻⁹ and shell model diagonalization.^{10,11} All these studies are based on the cranking model.

The cranking model, however, was pointed out to give inadequate results in the band-crossing region.¹²⁻¹⁴ Some authors applied improved approaches such as the particle-rotor model^{15,16} to the band-crossing phenomena. There is a remarkable variation in the pairing correlations when the angular momenta suddenly align in the band-crossing region. The alignment has a possibility to happen repeatedly in some nuclei as the rotational frequency ω increases. It is, therefore, desirable to investigate the variation of the pairing correlations by a method which is free from the drawback of the cranking model.

In this paper, we investigate the variation of the pairing correlations induced by the nuclear rotation by means of the particle-rotor model as well as the cranking model. The relation between the particle-rotor model and the cranking model has not necessarily been made clear. We examine it by comparing the two models through the Tanaka-Suekane method¹⁷ which was proposed to improve the HFB treatment of the cranking model. This study aims to offer an estimation of the efficiency of the cranking model for the pairing problem.

Our study is made in the single- j shell model space with $j = \frac{13}{2}$. We exactly diagonalize the two types of

model Hamiltonian; the cranking model Hamiltonian and the particle-rotor model Hamiltonian. We investigate the structure-variation of the wave functions depending on the rotational frequency ω and also on the angular momentum I in detail. The wave functions are analyzed in terms of the seniority starting from the basis states of $\omega=0$. The properties of the first excited band are also investigated. It should be noticed that our treatment is free from the defect of the static number-non-conserving pairing field approximation.

II. MODEL AND TREATMENT

We employ the single- j shell model space with $j = \frac{13}{2}$ in the axially symmetric Nilsson potential to consider the competition between the pairing correlations and the nuclear rotation. We start with the cranking model Hamiltonian

$$H_{cr} = H_{intr} - \omega J_x, \tag{1}$$

$$H_{intr} = \sum_{k\sigma} \kappa \frac{3k^2 - j(j+1)}{j(j+1)} c_{k\sigma}^\dagger c_{k\sigma} - G \sum_{kk'} c_{k+}^\dagger c_{k-}^\dagger c_{k'-} c_{k'+}, \tag{2}$$

$$J_x = \sum_{kk'} \langle k | j_x | k' \rangle (c_{k+}^\dagger c_{k'+} - c_{k-}^\dagger c_{k'-}). \tag{3}$$

Here k is the z component of the angular momentum of the particle, σ is the signature ($\sigma = \pm i$) and G is the pairing force strength. The energy is measured by an arbitrary energy unit κ .

The Hamiltonian of the particle-rotor model, on the other hand, is approximated by

$$H_{pr} = \frac{1}{2\mathfrak{I}} (I - J_x)^2 + H_{intr}, \tag{4}$$

where I means the total angular momentum of the system composed of a rotor part and a particle part, and it is

treated as a continuous parameter in our calculation. We diagonalize H_{pr} in the whole single-particle space coupled to the rotor. We make a number-conserving treatment of H_{intr} , which does not allow for the exchange of particle pairs between the core and particle parts.

The particle-rotor Hamiltonian (4) should be compared with the following Hamiltonian of the total system instead of H_{cr} :

$$H_{\text{tot}} = \frac{1}{2} \mathfrak{I} \omega^2 + H_{\text{intr}} . \quad (5)$$

We suppose that such a rotor-plus-particle system corresponds to the cranking model in this paper. The moment of inertia \mathfrak{I} is regarded to come from the collective rotor part and the same value is used for both \mathfrak{I} in (4) and in (5). In the cranking model, the total angular momentum I is given by

$$I \approx \omega \mathfrak{I} + \langle J_x \rangle . \quad (6)$$

This relation imposes the constraint condition under which the cranking model Hamiltonian H_{cr} is diagonalized. Various quantities are calculated as functions of ω in the cranking model. The translation from the ω dependence to the I dependence is made through the rela-

tion (6). Contrary to this, the rotational frequency ω does not appear in the particle-rotor model. If we want to get ω in the particle-rotor model, we can use the relation (6).

The basis states which are employed to diagonalize H_{cr} or H_{pr} are constructed in the following way. The degrees of freedom of a particle can be divided into two parts¹⁸,

$$c_{k\sigma}^\dagger = a_{k\sigma}^\dagger + \sigma S_k^\dagger a_{k\bar{\sigma}} , \quad (7)$$

$$S_k^\dagger = \sigma c_{k\sigma}^\dagger c_{k\bar{\sigma}}^\dagger , \quad a_{k\sigma}^\dagger = c_{k\sigma}^\dagger (1 - c_{k\bar{\sigma}}^\dagger c_{k\bar{\sigma}}) , \quad (8)$$

where S_k^\dagger represents the pairing degrees of freedom and $a_{k\sigma}^\dagger$ represents the others. The intrinsic Hamiltonian H_{intr} is then written as

$$H_{\text{intr}} = H_S + H_a , \quad (9)$$

$$H_S = \sum_k 2\epsilon_k N_k - G \sum_{kk'} S_k^\dagger S_{k'} , \quad (10)$$

$$H_a = \sum_k \epsilon_k v_k . \quad (11)$$

As H_S and H_a commute, the eigenstates of H_{intr} are the products of the eigenstates of H_S and those of H_a , which are written as

$$|v, N\gamma[k_1 k_2 \cdots]\rangle = a_{k_1\sigma_1}^\dagger a_{k_2\sigma_2}^\dagger \cdots |N\gamma[k_1 k_2 \cdots]\rangle , \quad (12)$$

$$|N\gamma[k_1 k_2 \cdots]\rangle = \sum_{\alpha_1 \alpha_2 \cdots \mathcal{D}[k_1 k_2 \cdots]} f_\gamma(\alpha_1 \alpha_2 \cdots \alpha_N) S_{\alpha_1}^\dagger S_{\alpha_2}^\dagger \cdots S_{\alpha_N}^\dagger |0\rangle . \quad (13)$$

Here, N is the number of the pairs S_k^\dagger , v is the number of unpaired nucleons (i.e., the seniority) and γ in (13) is the label of the order in energy, e.g., $\gamma=0$ corresponds to the lowest-energy state (the pairing field when $\omega=0$), $\gamma=1$ to the next lowest-energy state and so on. The symbol $[k_1 k_2 \cdots]$ means that the single particle levels listed in $[\]$ are blocked by unpaired nucleons $a_{k\sigma}^\dagger$. The blocked levels must be removed when we diagonalize H_S . The eigenstates of the Hamiltonian (1) or (4) are written as

$$|v + 2N, \mu(\omega \text{ or } I)\rangle = \sum_{v, N\gamma k_1 k_2 \cdots} g_\mu(v, N\gamma[k_1 k_2 \cdots](\omega \text{ or } I)) |v, N\gamma[k_1 k_2 \cdots]\rangle , \quad (14)$$

where μ is the label of the order in energy as the same notation as γ . In (14), the parameter ω is used for the cranking model and the parameter I is used for the particle-rotor model. The relation between the cranking model and the particle-rotor model is also investigated through the Tanaka-Suekane method in this paper. The Tanaka-Suekane method divides the cranking term into two parts, the seniority-conserving one and the seniority-changing one,

$$\omega J_x = \omega J_x^S + \omega J_x^A , \quad (15)$$

$$J_x^S = \sum_{kk'} \langle k | j_x | k' \rangle \sum_{\sigma} \sigma (a_{k\sigma}^\dagger a_{k'\sigma} + S_k^\dagger a_{k'\sigma}^\dagger a_{k\sigma} S_k) , \quad (16)$$

$$J_x^A = \sum_{kk'} \langle k | j_x | k' \rangle \sum_{\sigma} (a_{k\sigma}^\dagger a_{k'\bar{\sigma}}^\dagger S_k + S_k^\dagger a_{k\bar{\sigma}} a_{k'\sigma}) . \quad (17)$$

The first step of the Tanaka-Suekane method is to diagonalize H_{cr} excluding the seniority-changing part of the

cranking term ωJ_x^A and to select the lowest $v=0$ state and the lowest $v=2$ state. In the next step, the particle-rotor Hamiltonian (4) is diagonalized between the selected two states with the same I . This method is capable of overcoming the band-crossing anomaly of the cranking model. We compare the results of the Tanaka-Suekane method with those of the cranking model and particle-rotor model.

Our Hamiltonians have the parameters G , \mathfrak{I} , and the number of particles $v + 2N$. These values are set to simulate the values used in Ref. 12, i.e., $G/\kappa=0.207$, $\mathfrak{I}\kappa/\hbar^2=60$ and $v + 2N=4$ in the following calculations.

III. RESULTS AND DISCUSSIONS

In the cranking model, the diagram of the rotational frequency ω versus angular momentum I is used to translate various quantities in the rotating frame into

those in the laboratory frame, where the behavior of the quantities depending on I is observed in experiments. Therefore, the ω - I diagram is the key diagram in the cranking model.

Figure 1 shows the ω - I diagram for the yrast band obtained by our diagonalization method. The result of the cranking model is compared with that of the particle-rotor model. The resultant ω - I relation obtained by the Tanaka-Suekane method is also shown for a reference. The Tanaka-Suekane method was proposed to improve the drawback of the cranking model in the vicinity of the diabolical point where two bands cross each other. At that point, according to the usual explanation, the abrupt alignment of angular momenta of the particles causes a temporary decrease of the rotational frequency ω of the rotor. This situation is well understood by Fig. 1; while the cranking model shows only the gradual increase of ω during the alignment, the Tanaka-Suekane method describes the temporary decrease of ω from $I=10$ to $I=14$. Figure 1 indicates that the particle-rotor model can also describe the temporary decrease of ω from $I=10$ to $I=14$. Although the cranking model has the above drawback, it is still reliable apart from the diabolic point of the band crossing. Just at regions where ω is small or large enough in Fig. 1, the particle-rotor model reproduces the result of the cranking model. The result of the Tanaka-Suekane method, however, does not coincide with the other two at large ω .

We can hence conclude from Fig. 1 that the particle-rotor model is the most reliable one among these three approaches. This is also confirmed by the graph of the energies E_I for the yrast band, which is shown in Fig. 1 of our previous work.²¹ The cranking model cannot produce any bend in energy curve corresponding to the backbending of the moment of inertia. On the other hand, the particle-rotor model can produce it as the

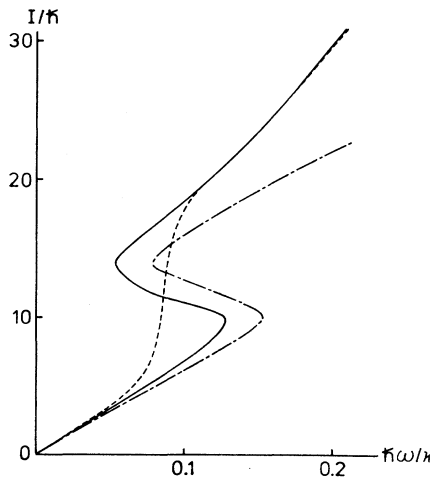


FIG. 1. Three ω - I relations for the yrast band are plotted. The dotted line corresponds to the resultant ω - I relation of the cranking model, the dash-dotted line corresponds to that of the Tanaka-Suekane method, and the solid line corresponds to that of the particle-rotor model.

Tanaka-Suekane method. In this way, we can say that the particle-rotor model is reliable in the whole region of I .

Our interest is the structure-variation of the wave functions which is induced by the nuclear rotation. Let us trace the variation shown in Fig. 1. We lay stress on the variation of the pairing correlations during the alignment and also on the increase of the angular momentum after the alignment.

The seniority structures of the yrast band are shown in Fig. 2. These lines show the mixing ratios of the basis states with respective seniority ν , i.e., $\sum (g_\mu)^2$ in terms of the factors g_μ defined in (14). In this figure, the result of the particle-rotor model reveals the rapid breaking of one particle-pair aligning their angular momenta from $I=10$ to $I=14$. Contrary to this, the result of the cranking model shows a gradual breaking of one particle pair in the wide range of I .

This figure shows the abrupt crossing of two "bands" characterized by $\nu=0$ and $\nu=2$ around $I=12$. We cannot, however, find any signs of the abrupt crossing of "bands" characterized by $\nu=2$ and $\nu=4$ in the region of $I=0\sim 30$ but see only a gradual increase of the mixture of these two bands. The second backbending, therefore, cannot be expected in our simple model. Actually, the ω - I diagram of Fig. 1 does not show any sign of the second backbending.

In our exact diagonalization in the full space, all the basis states of (14) are included in the wave functions. Both the static and dynamical contributions of the pairing correlations are included without any distinction in the results shown in Fig. 2. In order to analyze the roles of these two contributions, we made some calculations in a few cases in which we employed different ways of truncation when we diagonalized the Hamiltonian (1) or (4). In case I, we took $\gamma=0$ and 1 components in the basis states for the $\nu=0$ and took only $\gamma=0$ for $\nu=2$ states. In case II, we took $\gamma=0$ and 1 components for both $\nu=0$ and $\nu=2$ states. In case III, we took every component for $\nu=0$ and $\nu=2$ states but truncated the $\nu=4$ states. (Note that only $\gamma=0$ is allowed for $\nu=4$ states in the

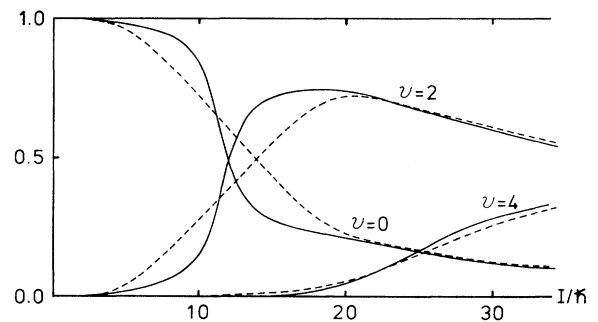


FIG. 2. The seniority structures of the yrast band obtained by the diagonalization of the cranking model Hamiltonian (dashed lines) and by that of the particle-rotor model Hamiltonian (solid lines) without any truncation.

four-particle system under consideration.) The resultant spin alignments of the yrast band obtained by the three types of truncations are shown in Fig. 3. Here we show the variation of ω in the cranking model because it is the most familiar diagram.

The result of case III in which the $v=4$ components are excluded indicates that, without the $v=4$ components, angular momenta of the particles do not increase sufficiently at large ω . This is the reason why the result of the Tanaka-Suekane method cannot catch up with those of the other two results at large ω in the diagram of $\omega-I$ (Fig. 1). The Tanaka-Suekane method contains only the lowest states for each $v=0$ or 2. The decoupling of one pair cannot produce the angular momentum more than $I \sim 12$, which results in the saturation of $\langle J_x \rangle$ (see also Fig. 1). The decoupling of another pair is necessary to gain higher spin.

This decoupling of the two pairs, however, is not induced if we do not include the $\gamma=1$ component into the $v=2$ states when we diagonalize the cranking term, which can also be seen in Fig. 3. The curve of case I shows the saturation of $\langle J_x \rangle$ value at large ω . This means that the $v=4$ states get mixed into the ground-band state through the coupling with the $\gamma=1$ components of the $v=2$ states. In fact, if we include the $\gamma=1$ components in the $v=2$ states (case II), we can get sufficient increase of the value $\langle J_x \rangle$ at large ω and can qualitatively reproduce the result of the full-space diagonalization.

The facts stated above lead us to conclude that the ωJ_x^A part of the cranking term which was neglected in the Tanaka-Suekane method becomes important after the band crossing. The ωJ_x^A term admixes the $\gamma \geq 1$ components of low-seniority states and it induces the high-seniority components to mix into the wave functions of the ground-band states. It may be possible to make the

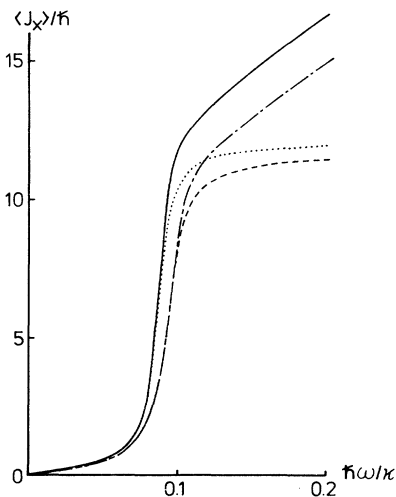


FIG. 3. Variation of the spin alignments of the yrast band. The results obtained by the three types of the truncation; cases I, II, and III (see the text); are compared with the result obtained without any truncation.

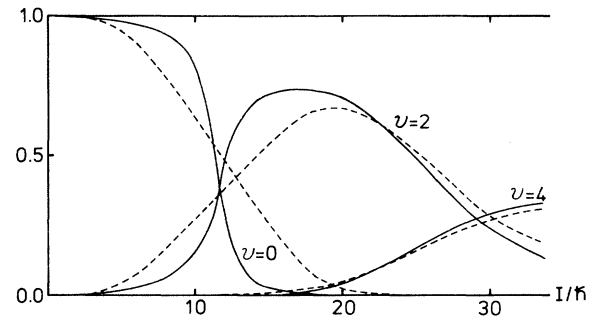


FIG. 4. Same as Fig. 2 except that only the $\gamma=0$ components for $v=0, 2$, and 4 states are added together.

following correspondences: The $\gamma=0$ states of $v=0, 2$, and 4 are constructed on the "static pairing field" and the $\gamma=1$ states of them include "pairing vibrations" as the fluctuation of the field. In this language, the above results mean that the cranking term makes the particle-pairs decoupled (and aligned), and at the same time, it makes the pairing field fluctuate.

The importance of the pairing vibrations can be understood from Fig. 4, in which the squared amplitudes of only the $\gamma=0$ components of respective v in the full diagonalization are plotted. The comparison between Fig. 2 and 4 tells us that the pairing vibrational states with $v=0$ and 2 are important at large I . The result of case II in Fig. 3 indicates the special importance of the first ($\gamma=1$) pairing vibrational state. It is also suggested by Fig. 4 that the second backbending due to a drastic band crossing does not occur at $I \geq 14$.

Let us now attend to the value $\bar{\Delta} \equiv G\sqrt{\langle S^\dagger S \rangle}$ as a measure of the pairing correlations.^{3,19,20} Figure 5 plots the I dependence of $\bar{\Delta}/G$ calculated by the cranking model and the particle-rotor model in case I, in case II, and in the full diagonalization.

The first point we notice is that the curve of $I-\bar{\Delta}$ obtained by the cranking model does not show a sharp decrease in the band crossing region and this situation is different from that usually drawn in the graph of $\omega-\bar{\Delta}$. This is due to the failure of the cranking model in the description of the band crossing. Contrary to this, the particle-rotor model is capable of describing the rapid decrease of the pairing correlation energy from $I=10$ to $I=12$ which is related to the decoupling (and alignment) of one particle pair. We have reported the same situation about the so-called diabolic pair transfer.²¹

We can also see from Fig. 5 that the inclusion of the pairing vibrational components is indispensable for obtaining a correct value of $\bar{\Delta}$ after the band crossing. As discussed above, the states with the pairing vibrations induce the mixing of $v=4$ states (i.e., the breaking of two particle pairs) through the effect of ωJ_x^A term. It is notable that the inclusion of the lowest pairing vibrational component of the respective states with seniorities $v=0$ and 2 is almost sufficient to reproduce the results of the full diagonalization. The fluctuations of the pairing field can roughly be compensated by including the lowest pairing vibrational components.

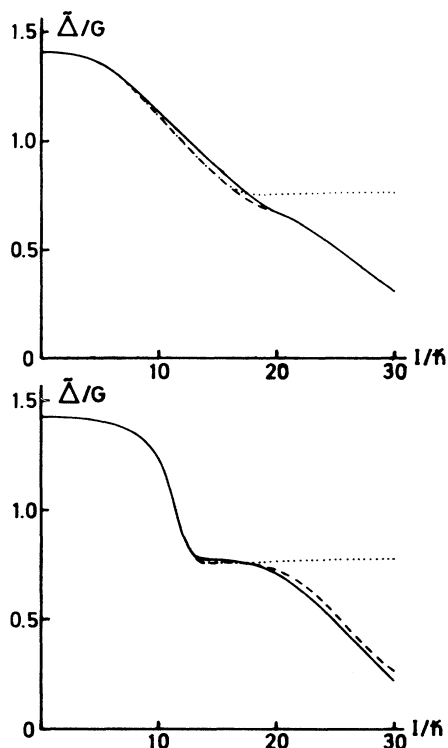


FIG. 5. The angular momentum dependence of the pairing gap ($\tilde{\Delta}/G$). The upper part shows that of the cranking model and the lower part shows that of the particle-rotor model. The dotted lines, dashed lines, and the solid lines correspond to the results of case I, case II, and the full diagonalization, respectively.

Because there is no second backbending in our model, $\tilde{\Delta}$ does not show a drastic change at large I in Fig. 5. We should expect more complicated situations in realistic cases. As also seen in Fig. 5, $\tilde{\Delta}$ becomes very small at very high spin I . This means the breaking of most particle pairs, which suggests the pairing collapse predicted by Mottelson and Valatin.²² It should, however, be noticed that this collapse is retarded in the graph of $I\tilde{\Delta}$ as compared with that in the usual graph of $\omega\Delta(\text{gap})$. The exact diagonalization of the pairing force, which takes account of the fluctuations of the pairing field, does not bring about the abrupt disappearance of "gap" in contrast with the HFB (or BCS) approximation.

The structure of excited bands has been discussed by some authors^{11,23} using the cranking model. The comparison between the cranking model and the particle-rotor model reveals an important discrepancy for the yrast band, as shown in the above discussions. It is interesting to investigate the excited bands by the two models.

Figure 6 is the ω - I diagram for the first-excited band. The graph of the particle-rotor model displays strange behavior in the vicinity of $\omega=0$ ($0 \leq I \leq 6$), but after that, it shows a monotonous increase. It should be noticed that this graph is a single-valued function of I . Contrary to this, the curve obtained by the cranking model is very strange in the band-crossing region. The graph is a mul-

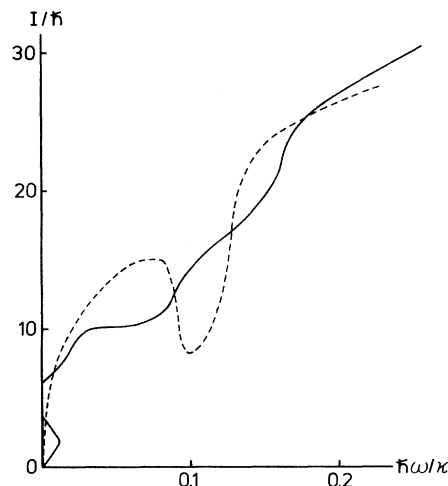


FIG. 6. The ω - I relations for the first excited band. The solid line shows that obtained by particle-rotor model and the dashed line shows that of the cranking model.

tivalued function of I , which makes it impossible to fix the rotational frequency ω for each I state. While the respective states with the same I of the yrast and first-excited bands are orthogonal to each other in the particle-rotor model, the respective states of both bands in the cranking model are made orthogonal at the same ω but not at the same I . Accordingly, the cranking model is not necessarily appropriate to the description of the excited bands.

The seniority structure of the first-excited band calculated by the particle-rotor model is illustrated in Fig. 7. This figure indicates that the main components of the first-excited band state are still the $\nu=2$ ones at high-spin I . Figure 7 is considerably different from the corresponding figure (plotted by ω) presented by Wu *et al.*^{11,23} using the cranking model. The present results suggest that a careful treatment of the cranking model for the excited bands is necessary.

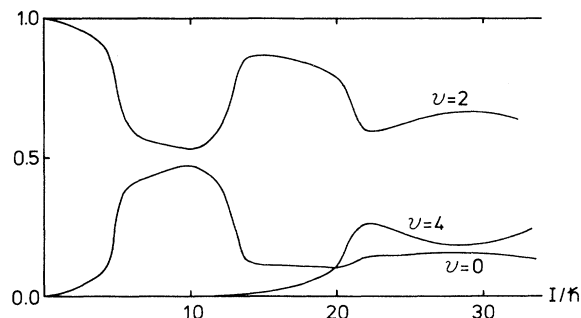


FIG. 7. The seniority structure of the first excited band obtained by the diagonalization of the particle-rotor model Hamiltonian without any truncation.

IV. CONCLUSIONS

We have investigated the variation of the structure of the rotor-plus-particle system laying particular stress on the relation between the pairing correlations and the nuclear rotation. The wave functions are calculated by the exact diagonalizations of the Hamiltonians in the cranking model and in the particle-rotor model.

We compared these two models through the Tanaka-Suekane method which was proposed to treat appropriately the band-crossing region based on the cranked HFB method. The comparison tells us that the particle-rotor model is reliable in all the regions of angular momentum I . The particle-rotor model properly describes the decoupling and alignment of one particle-pair in the band-crossing region, while the cranking model fails to describe it. After the band-crossing region, the angular momenta of particles increase steadily, which is seen in both of the two models; in the cranking model and in the particle-rotor model. This steady increase is due to the mixing of the seniority $\nu=4$ components relevant to the decoupling of two particle-pairs.

According to the analysis of the wave functions of the yrast states, the band crossing is caused fundamentally by the inversion of the energy order between the lowest $\nu=0$ state and the lowest $\nu=2$ state. After the band crossing, however, the fluctuations of the static pairing field play important roles to gain large angular momentum. This is described by the remarkable mixing of pairing vibrational $\nu=0$ and $\nu=2$ components in the ground-band states. We have learned that the $\nu=2$ states with the lowest pairing vibrational component induce the mixing of the $\nu=4$ states. The qualitative aspect of our model can be

reproduced in the truncated space where the respective lowest two states ($\gamma=0$ and 1) of $\nu=0$ and $\nu=2$ are taken into account in addition to the $\nu=4$ states.

We calculated the values $\bar{\Delta} \equiv G\sqrt{\langle S^\dagger S \rangle}$ as a measure of the pairing interaction in our exact treatment of the pairing correlations. The curve of $I\bar{\Delta}$ reflects the variations of the pairing correlations caused by the nuclear rotation. The value $\bar{\Delta}$ obtained by the particle-rotor model decreases abruptly at $I \sim 12$. This abrupt decrease of $\bar{\Delta}$ is not seen in the cranking model but is seen only as a gradual decrease. At very high spin, $\bar{\Delta}$ becomes very small but does not disappear so soon in contrary to the prediction of the HFB (or BCS) approximation. This fact also indicates the importance of the pairing vibrational motion, i.e., fluctuations of the static pairing field as discussed by others.^{8,9}

The structure of the first-excited band is analyzed by the cranking model and particle-rotor model. In the calculated results of the cranking model, it seems that the defect of the nonorthogonality of the excited- and ground-band states with the same I is disclosed. The diagram of $\omega-I$ becomes multivalued with respect to I in the cranking model while that in the particle-rotor model is reasonable. The wave functions of the excited states in the cranking model are not so reliable but must be carefully applied to the evaluation of physical quantities.

ACKNOWLEDGMENTS

We would like to thank Mr. Horinouchi for his help during the preparation of the manuscript. The numerical calculations were carried out by using FACOM M780/10S at Computer Center, Fukuoka University.

¹L. F. Canto, P. Ring, and J. O. Rasmussen, Phys. Lett. **161B**, 21 (1985).

²W. Satuła, W. Nazarewicz, Z. Szymański, and R. Piepenbrink, Phys. Rev. C **41**, 298 (1990).

³J. L. Egido and P. Ring, Nucl. Phys. **A383**, 189 (1982); **A388**, 19 (1982).

⁴W. Nazarewicz, J. Dudek, and Z. Szymański, Nucl. Phys. **A436**, 139 (1985).

⁵R. S. Nikam, P. Ring, and L. F. Canto, Phys. Lett. **185B**, 269 (1987).

⁶R. A. Broglia and M. Gallardo, Nucl. Phys. **A447**, 489 (1985).

⁷D. R. Bes, R. A. Broglia, J. Dudek, W. Nazarewicz, and S. Szymański, Ann. Phys. (N.Y.) **182**, 237 (1989).

⁸Y. R. Shimizu, J. D. Garrett, R. A. Broglia, M. Gallardo, and E. Vigezzi, Rev. Mod. Phys. **61**, 131 (1989).

⁹Y. R. Shimizu and R. A. Broglia, Nucl. Phys. **A515**, 38 (1990).

¹⁰J. A. Sheikh, M. A. Nagarajan, N. Rowley, and K. F. Pál, Phys. Lett. **B223**, 1 (1989).

¹¹C. S. Wu and J. Y. Zeng, Phys. Rev. C **40**, 998 (1989).

¹²I. Hamamoto, Nucl. Phys. **A271**, 15 (1976).

¹³E. R. Marshalek and A. L. Goodman, Nucl. Phys. **A294**, 92 (1978).

¹⁴F. Grümmer, K. W. Schmid, and A. Faessler, Nucl. Phys. **A308**, 77 (1978).

¹⁵F. Grümmer, K. W. Schmid, and A. Faessler, Nucl. Phys. **A317**, 287 (1979).

¹⁶C. G. Anderson and J. Krumlinde, Nucl. Phys. **A334**, 486 (1980).

¹⁷Y. Tanaka and S. Suekane, Prog. Theor. Phys. **66**, 1639 (1981).

¹⁸M. Hasegawa and S. Tazaki, Phys. Rev. C **35**, 1508 (1987).

¹⁹R. Bengtsson and H. B. Håkansson, Nucl. Phys. **A357**, 61 (1981).

²⁰P. Ring and P. Schuck, *The Nuclear Many-Body Problem* (Springer, New York, 1980).

²¹M. Hasegawa, S. Tazaki, and K. Muramatsu, Phys. Lett. **B226**, 1 (1989).

²²B. R. Mottelson and J. G. Valatin, Phys. Rev. Lett. **5**, 511 (1960).

²³J. Y. Zeng, C. S. Wu, L. Cheng, and C. Z. Lin, Phys. Rev. C **41**, 2911 (1990).